Voltage-Based Physical Layer Fault Diagnosis for Controller Area Network

Alaeddin Bani Milhim[1], Hadyan Ramadhan[2], Hamed Kazemi[3], Xinyu Du[4], Shengbing Jiang[5], and Hossein Sadjadi[6]

[1,2,3,6]*General Motors Canadian Technical Centre, Markham, Ontario, L3R 4H8, Canada*

alaeddin.banimilhim@gm.com
hadyan.ramadhan@gm.com
hamed.kazemi@gm.com
hossein.sadjadi@gm.com

[4,5]*General Motors Global Technical Center, Warren, Michigan, 78092, USA*

xinyu.du@gm.com
shengbing.jiang@gm.com

ABSTRACT

Controller Area Network (CAN) is the most prevalent communication protocol used in the automotive industry. This in-vehicle network provides a means for communication between Electronic Control Units (ECUs) and components within the vehicle. The recent rapid development of connected, electric, and autonomous vehicles, expands the complexity and information exchange within CAN and demands an increase in the reliability of the network. Efficient system-level diagnosis functions need to be integrated over the network to ensure reliability and enhance the ease of troubleshooting.

This paper presents a method to identify physical CAN faults such as loss of electrical connections and shorted wires. Fault signatures of predefined physical CAN faults are used to detect and identify the failure modes. The method can identify both permanent and intermittent faults caused by, for instance, damaged connectors and vibrations, respectively.

Diagnosis tasks are implemented on an in-vehicle module by measuring and processing physical layer voltages of all CAN buses. A real-time data buffer of a predefined size is utilized to calculate health indicators from the physical layer CAN voltages. The health indicators are then compared to predefined thresholds to determine the presence and identify the type of the fault. Compared to ground truth data, the results show that the presented method can identify with high accuracy physical CAN faults including open electrical connection and shorted wires.

1. INTRODUCTION

Controller Area Network (CAN) communication networks are widely used for in-vehicle communications (ISO, 1993). Different types of physical faults can occur in CAN communication networks such as single or dual CAN wire open, CAN wire short (i.e., short between CAN Hi and CAN Lo, and shorted to power or ground). The correct detection and diagnosis of CAN bus faults is critical for the successful control of the vehicle. Different approaches have been developed for CAN bus fault detection and diagnosis (For example, see Xiao and Lei (2013), Mary, Alex, and Jenkins (2013), Asaduzzaman, Bhowmick, and Moniruzzaman (2014), Farsi, Ratcliff, and Barbosa (1999), Robertson (2014), Hu and Qin (2011), Kelkar and Kamal (2014), Lei, Yuan, and Zhao (2014), Wheeler, Timucin, Twombly, Goebel, and Wysocki (2007), Furse, Smith, Safavi, and Lo (2005), Furse, Chung, Lo, and Pendalaya (2006)).

One of the main CAN bus fault detection and diagnostic approaches is based on CAN message monitoring, such as the typical method called signal supervision that is used in several production vehicles (Furse, Smith, Safavi, and Lo (2005)). In order to detect any communication fault, the method of signal supervision is usually adopted at the receiver side. For example, suppose a signal A is sent out periodically by some sender ECU X every T time unit. If the receiver ECU Y does not receive any updated signal A for N*T time units, then ECU Y can declare a loss of signal A from ECU X, in which case a Diagnostic Trouble Code (DTC) U-code could be set by the receiver Y to indicate the loss of communication with the sender ECU X. In the above, N is a calibratable number (normally N=2.5, but can be high for robustness), and is used to exclude some transient faults from communication jitter or random noises.

The above DTC U-codes have some limitations. First, a DTC U-code only indicates the loss of communication between ECUs that are designed to transmit/receive direct messages between them. It cannot tell where the fault is, nor what type of physical fault it is. Second, for intermittent faults, when a fault occurs, the corresponding DTC U-code will be set with the status of "current". After the fault disappears and the system recovers, the status of the DTC U-code will be changed to "history". However, for the current DTC U-codes there is no time info to indicate when the fault occurred and when the fault recovered. Third, a fault in the communication network may result in multiple DTC U-codes set by multiple ECUs at separate times at which multiple ECUs point to communication faults at different ECUs. Fourth, for the dual-wire high speed CAN bus, a single wire open fault, either CAN Hi or CAN Lo wire open fault, on the CAN bus, which separates the network into two disconnected segments, may result in a DTC U-code for a sender ECU that is on the same segment as the receiver ECU as described in Furse et al. (2006).

To overcome the above limitations of DTC U-codes, an integrated software-based approach was developed in Furse et al. (2006) based on both message monitoring and system topology for detection and localization of the CAN communication faults. However, due to the limitations of message monitoring, the approach developed in Furse et al. (2006) cannot isolate different fault types such as CAN Hi/Lo single wire-open, shorted to power/ground, or wire short between CAN Hi and Lo. This is because those faults have the same symptoms by message monitoring. Therefore, they are indistinguishable by message monitoring alone.

Besides the message monitoring approaches, there are also physical signal measurement-based approaches, using voltage, current, and/or bit-time measurements (see Farsi et al. (1999), Robertson (2014), Hu and Qin (2011), Kelkar and Kamal (2014), Lei et al. (2014), Wheeler et al. (2007)). Some of those approaches monitor the bus passively, while others actively send out inquiries. Although those approaches have different successes for different cases, none of them provides a cost effective and accurate method for the diagnosis of different CAN bus wire faults.

In this paper, a new voltage-based approach for the diagnosis of CAN communication faults is presented. The main idea is to monitor both CAN Hi and Lo voltages, and diagnose bus wire faults based on the voltage patterns. The proposed approach has been implemented in an on-board ECU and tested using actual vehicle data. The test results show that the approach can successfully detect and diagnose different CAN bus wire faults.

2. PHYSICAL CAN BUS WIRE

The physical layer characteristics for the CAN bus are specified in ISO-11898-2. The physical layer of a high-speed CAN bus consists of pair wires, terminators at both side, and ECUs equipped with the CAN transceiver to receive and transmit messages. The schematic of a typical high-speed CAN bus is shown in Figure 1 where the bus has n-ECUs and split termination. Parallel wires with a nominal impedance of 120 Ω (95 Ω minimum and 140 Ω maximum) are normally utilized. A maximum length of 40 meters is specified for CAN at a data rate of 1 Mb (ISO, 1993)

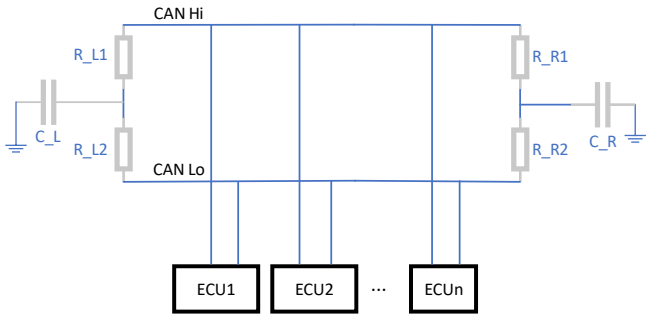

Figure 1. The schematics for a typical high-speed CAN bus.

At lower data rates, longer wires are possible as well. The two signal lines of the bus are called CAN Hi and CAN Lo. In the recessive state, the bus voltages are equal to 2.5 V. The dominant state on the bus typically drives the CAN Hi up to 3.5 V, and CAN Lo down to 1.5 V, creating a 2 V differential signal. Figure 2 shows the normal CAN voltage profile with sampling rate of 10 msec.

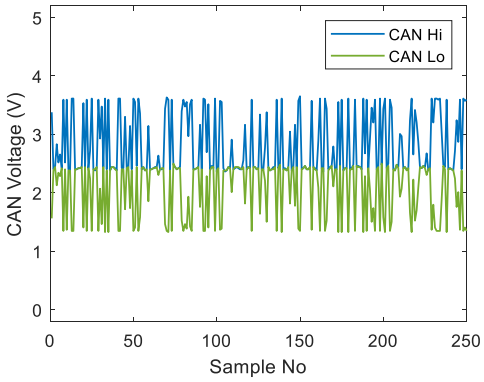

Figure 2. CAN bus voltage under normal conditions.

The bus terminations are placed at each end of the bus. Each terminator includes two resistors of approximately 60 Ω each and a coupling capacitor which couples high-frequency noise to a solid ground potential.

With the recent expansion of utilizing CAN for vehicular communication between devices, the CAN bus bandwidth usage became higher which led to migrate the network to CAN with flexible data rate (CAN FD). Classical CAN network would only allow 8 data bytes with data transfer speed of up to 1 MB/s. CAN FD bandwidth can support 5 MB/s with up to 64 data bytes in a single frame (Zago and Freitas (2018)).

3. CAN Bus Wire Faults

This paper presents a voltage-based approach to diagnose CAN physical layer faults. The method is based on evaluating the CAN voltage profile and determining if it matches with any of the predefined physical CAN fault signatures. Different physical layer faults have distinguishable voltage signatures, which are reflected by the health indicators and can be used to identify the fault types. To do so, these voltage signatures should be identified and analyzed. This work focuses on the following faults: single wire open, dual wire open, wire shorted to power, wire shorted to ground, and CAN Hi shorted to CAN Lo (Jiang, Du, and Wienckowski, (2015), Jiang, Du, and Nagose, (2015)).

CAN Hi and CAN Lo voltages are measured and processed on-board using the Central Gateway Module as the monitoring ECU. The voltage range of the measurements is between 0 V (lower limit) and 5 V (upper limit). If the measured CAN bus voltage is greater than the upper limit, a ceiling value of 5 V is applied by the monitoring ECU. The measurements are taken at a sampling rate of 10 Hz and stored in buffers of 250 samples each for processing. Once the buffer is filled, health indicators are calculated to determine whether a physical layer fault is present on the CAN bus.

3.1. Single Wire Open Fault

Figure 3 shows the trace of CAN bus voltage under single CAN Hi wire open fault. This fault type is characterized by the recessive CAN Hi and CAN Li voltages dropping to below 2 V. Identification of this type of fault can be done by counting the number of samples of CAN Hi voltage that drops below a certain threshold.

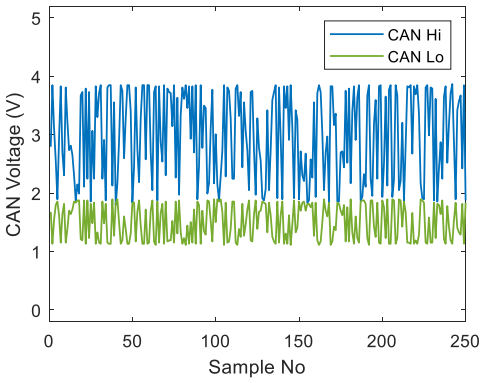

Figure 3. CAN bus voltage under single CAN Hi wire open fault.

Conversely to CAN Hi wire open fault, CAN Lo wire open fault is characterized by the recessive CAN Hi and CAN Lo voltages rising to above 3 V. The trace of CAN bus voltage under single CAN Lo wire open fault is shown in Figure 4. Counting the number of samples of CAN Lo voltage that rises above a certain threshold can be used to identify this type of fault.

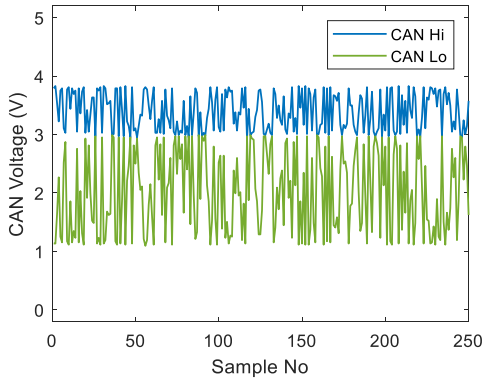

Figure 4. CAN bus voltage under single CAN Lo wire open fault.

3.2. Dual Wire Open Fault

Figure 5 shows the trace of CAN bus voltage under dual CAN Hi and CAN Lo wire open fault. Under this fault type, CAN Hi and CAN Lo voltages in the dominant state are slightly higher than 3.5 V and lower than 1.5 V, respectively. However, the overall measured voltage profile is similar to that without faults. As a result, identification of this type of fault is challenging from voltage measurements alone.

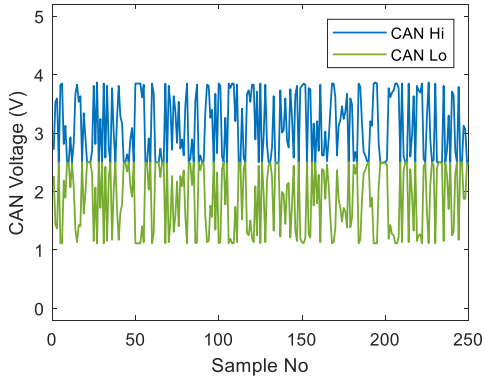

Figure 5. CAN bus voltage under dual CAN Hi and CAN Lo wire open fault.

3.3. Wire Shorted to Power Fault

Figure 6 shows the trace of CAN bus voltage under CAN Hi shorted to power fault. Under this fault type, the measured CAN Hi voltage is at the maximum value of 5 V. Majority of the measured CAN Lo voltage is also at the maximum value of 5 V with occasional drops to lower values between 3 V and 5 V. The drops can be attributed to the fact that some ECUs attempt to transmit on the bus while the fault is present.

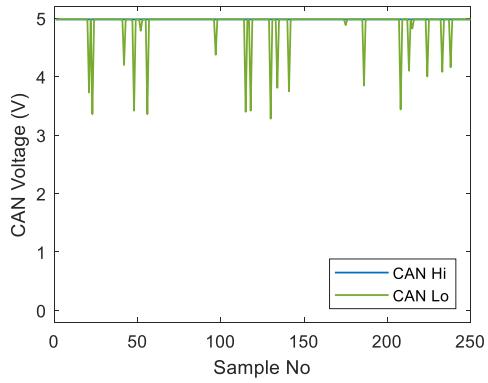

Figure 6. CAN bus voltage under CAN Hi shorted to power fault.

The trace of CAN bus voltage under CAN Lo shorted to power fault is shown in Figure 7. Under this type of fault, both CAN Hi and CAN Lo voltages are always at the maximum value of 5 V.

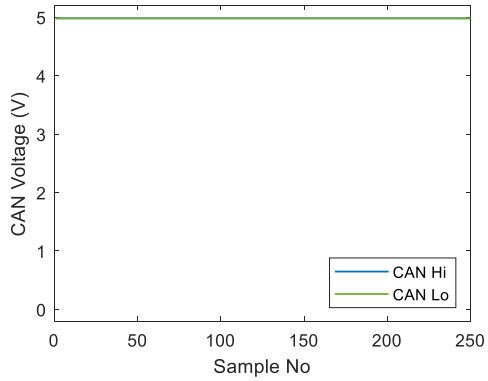

Figure 7. CAN bus voltage under CAN Lo shorted to power fault.

3.4. Wire Shorted to Ground Fault

Figure 8 shows the trace of CAN bus voltage under CAN Hi shorted to ground fault. Under this type of fault, both CAN Hi and CAN Lo voltages are always at the minimum value of 0 V.

Similar to CAN Hi shorted to power fault, CAN Lo shorted to ground fault results in CAN Lo voltages being set at the minimum level of 0 V, while CAN Hi voltages vary from 0 V to 3 V. The trace of CAN bus voltage under CAN Lo shorted to ground fault is shown in Figure 9.

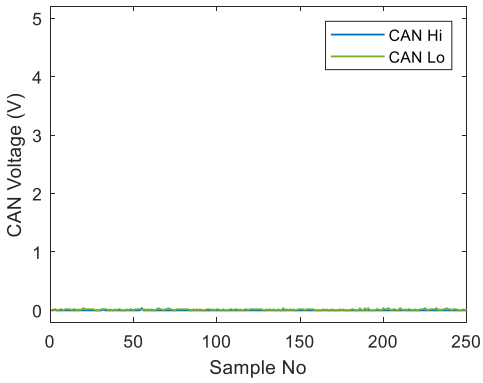

Figure 8. CAN bus voltage under CAN Hi shorted to ground fault.

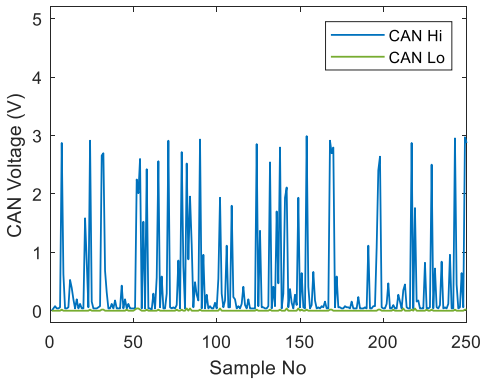

Figure 9. CAN bus voltage under CAN Lo shorted to ground fault.

3.5. CAN Hi Wire Shorted to CAN Lo Wire Fault

Under CAN Hi wire shorted to CAN Lo wire fault, both CAN Hi and CAN Lo voltages have measurements of around 2.5 V. The trace of CAN bus voltage under CAN Hi wire shorted to CAN Lo wire fault is shown in Figure 10. This voltage profile looks similar to that of idle CAN bus as there are no dominant voltages on the bus.

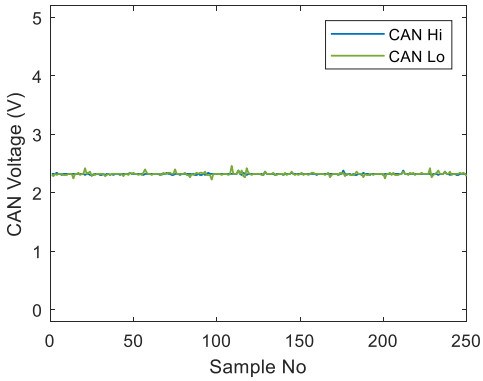

Figure 10. CAN bus voltage under CAN Hi wire shorted to CAN Lo wire fault.

4. VOLTAGE-BASED PHYSICAL CAN WIRE FAULT DIAGNOSTICS APPROACH

This section presents the proposed approach to diagnose physical CAN wire using voltage measurements. The voltage data is continuously collected even when the data is being processed. Therefore, this approach requires two sets of buffers: one for the data being processed and one for the data being collected. The flowchart of the presented method is shown in Figure 11. The sequential style is selected for this method to isolate the fault state as multiple fault state conditions can be met at same time. Therefore, the priority is assigned to the most estimated confident state. Moreover, the sequential style has the benefit on saving memory as evaluation the rest of the fault states is not required once the highest priority fault state is determined.

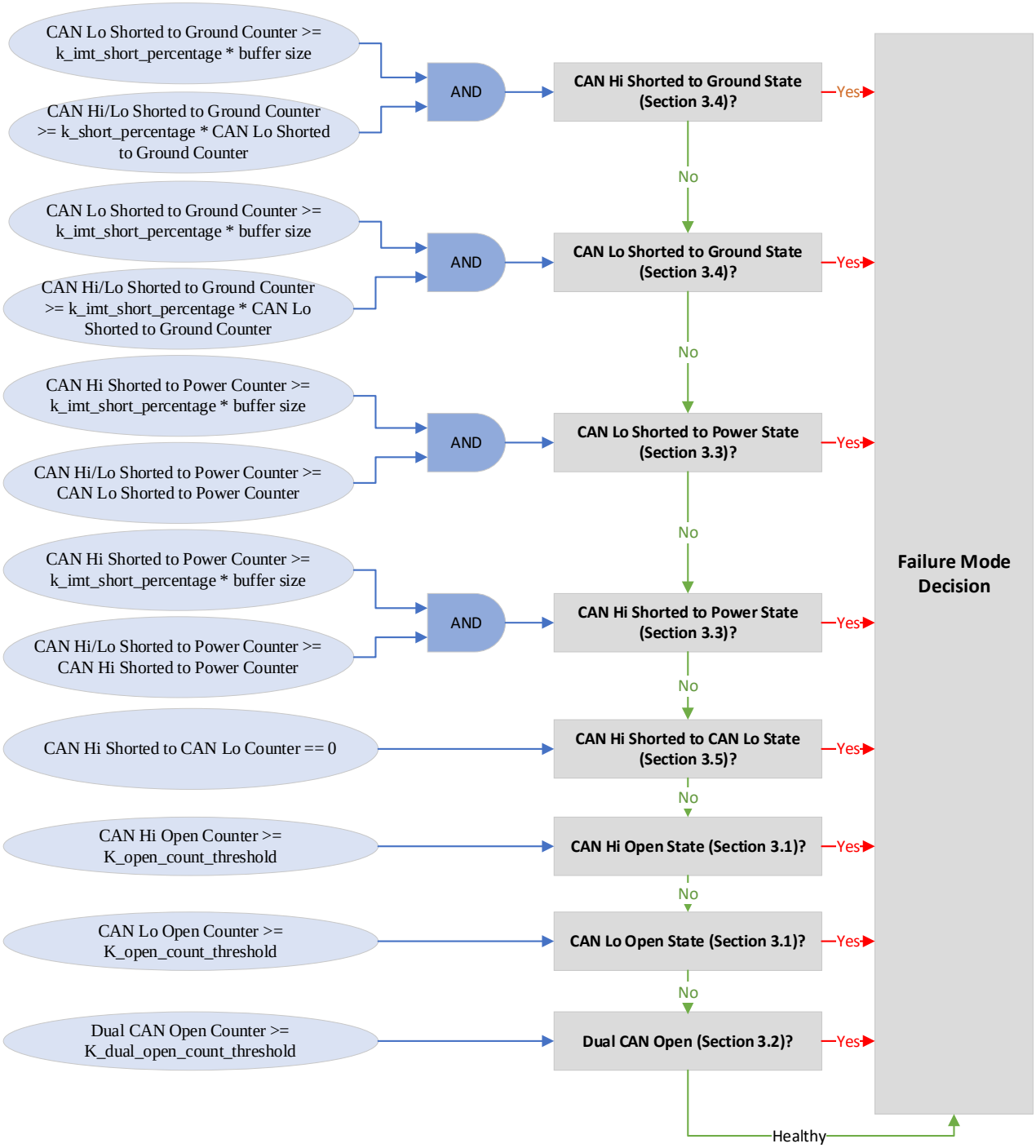

Figure 11. CAN fault state determination logic.

The algorithm is triggered after the vehicle is powered on by sometimes (e.g. 5 seconds) to allow the ECU communications to be stabilized. The presented logic is described in detail as follows.

For each CAN voltage pair within the buffer, perform the followings:

A. Count the number of times CAN Lo is greater than the recessive voltage level by a predefined threshold (k_single_open_threshold). This counter is referenced CAN Lo Open Counter.

B. Count the number of times CAN Hi is less than the recessive voltage level by a predefined threshold (k_single_open_threshold). This counter is referenced CAN Hi Open Counter.

C. Count the number of times CAN Lo is less than a predefined voltage threshold (k_short_ground_threshold). This counter is referenced as CAN Lo Shorted to Ground Counter.

D. Count the number of times both CAN Hi and CAN Lo are less than k_short_ground_threshold. This counter is referenced as CAN Hi/Lo Shorted to Ground Counter.

E. Count the number of times CAN Hi is greater than predefined voltage threshold (k_short_power_threshold). This counter is referenced as CAN Hi Shorted to Power Counter.

F. Count the number of times both CAN Hi and CAN Lo are greater than k_short_power_threshold. This counter is referenced as CAN Hi/Lo Shorted to Power Counter.

G. Count the number of times the difference between CAN Hi and CAN Lo is more than a predefined threshold (k_double_open_delta_threshold). This is referenced as Dual CAN Open Counter.

H. Count the number of times the difference between CAN Hi and CAN Lo is less than a predefined dominant threshold (k_dom_threshold). This is referenced as CAN Hi Shorted to CAN Lo Counter.

After the counters have been calculated for each buffer, the fault state is estimated based on the logic in Figure 11. Then, the decision will be made based on the state priority as shown in Figure 11. Therefore, the highest priority state will be reported, and the remaining states do not need to be evaluated. If none of the fault states is detected, the logic will report the CAN bus state as healthy.

The CAN physical layer fault diagnostic algorithm was calibrated using CAN bus voltage data from several production vehicles. The data was collected under normal as well as fault injected conditions. The default calibration values are listed in **Error! Reference source not found.**.

Calibratable Parameter	Value	Unit
k_single_open_threshold	324	mV
k_short_ground_threshold	646	mV
k_short_power_threshold	4500	mV
k_double_open_delta_threshold	2100	mV
k_dom_threshold	1474	mV
k_imt_short_percentage	5	Percentage
k_short_percentage	90	Percentage
k_open_count_threshold	2	Counter
k_dual_open_count_threshold	7	Counter
buffer_size	250	Counter

Table 1. Presented method calibration values

5. RESULTS AND DISCUSSIONS

Figure 12 shows the confusion matrix for the CAN physical layer fault diagnostic algorithm. Compared to the ground truth, the results show that the algorithm can identify single wire open, wire shorted to power, wire shorted to ground, and CAN Hi wire shorted to CAN Lo wire faults with high accuracy.

Single wire CAN Hi and CAN Lo open faults can be identified with true positive rates of 94.2% and 92.1%, respectively. As previously mentioned, identification of dual CAN open fault has a low rate due to its voltage signature resembling to that without faults. Consequently, the true positive rate for this type of fault is only 27.2%. The identification rate for the dual CAN open fault can be improved by considering multiple health indicators.

Identification of CAN Hi wire shorted to power fault has true positive rate of 63.4%. It is often misidentified as CAN Lo wire shorted to power fault due to the CAN Lo voltage not dropping to lower values in some instances.

The true positive rate for CAN Lo wire shorted to power, CAN Hi wire shorted to ground, and CAN Lo wire shorted to ground faults is 100%. The CAN Hi wire shorted to CAN Lo wire fault can be identified at 91.5% true positive rate with occasional misidentification as CAN Hi wire shorted to ground fault.

It is worth mentioning that the proposed method has 0% false positive rate under normal conditions as all healthy buffers are reported to be healthy. However, there are a few false negative scenarios. False positive leads to unnecessary maintenance while false negative leads to ignoring the faulty scenarios. It is recommended to be conservative for the false positive in this approach for CAN troubleshooting; so, misguidance can be avoided. False negative can be compensated by using other CAN diagnostics methods.

Different sets of vehicle data were used for validation purposes. It was found that the logic can function properly on several vehicle platforms with different ECU contents, with high identification rate.

summarizes the validation results.

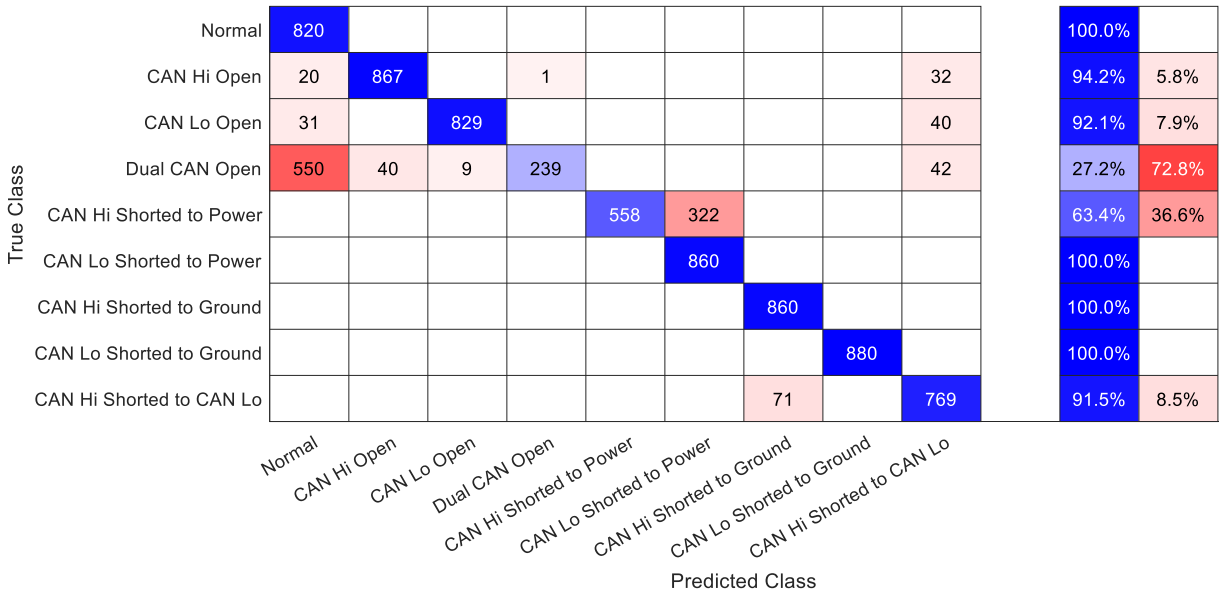

Figure 12. Confusion matrix for the CAN physical layer fault diagnostic algorithm.

It can be observed that the validation results match that of the calibration. This suggests that the calibration values used in the development and calibration processes are insensitive to the vehicle platforms and/or ECU contents.

Any other CAN fault type does not fit in the studied fault types while resulting in CAN communication disruption, it will be reported as unknown. So, other available CAN diagnostic methods can be leveraged for troubleshooting.

Injected fault state	Test number	Detection rate
CAN Hi Short to Ground	1000	100%
CAN Lo Short to Ground	1020	100%
CAN Hi Short to Power	1030	63%
CAN Lo Short to Power	970	100%
CAN Hi Short to CAN Lo	980	92%
CAN Hi Open	1070	92%
CAN Lo Open	1099	84%
Dual CAN Open	966	25%

Table 2. Validation results of the proposed method

6. CONCLUSIONS

This paper presents a method to identify CAN physical fault types. The method relies on raw CAN voltage measurements to classify the CAN voltage profiles. Performance of the method was evaluated using actual vehicle data. The results showed that the proposed approach can provide with high accuracy identification of physical CAN fault types. The method was calibrated and validated using over 8000 sets of vehicle data. It is recommended to expand this approach to cover other types of physical CAN fault as well as to investigate the potential use of proposed method for other communication protocols such as Ethernet.

REFERENCES

International Organization for Standardization, (1993). Road Vehicles— Interchange of Digital Information—Controller Area Network (CAN) for High-Speed Communication, *ISO/DIS Standard 11898:1993*

Xiao H. and Lei Y., (2013). Data Driven Root Cause Analysis for Intermittent Connection Faults in Controller Area Networks, *in Chinese Automation Congress, Changsha, China, pp. 300-305*

Mary G., Alex Z., and Jenkins L., (2013). Reliability Analysis of Controller Area Network Based Systems - a review, Int. J. Communications, Network and System Sciences, Vol.6 No.4, pp. 155-166

Asaduzzaman A., Bhowmick S., and Moniruzzaman M., (2014). Design and Evaluation of Controller Area Network for Automotive Applications, American Journal of Embedded Systems and Applications, Vol. 2, No. 29, pp. 29-37

Farsi M., Ratcliff K., and Barbosa M., (1999) An overview of Controller Area Network, Computing & Control Engineering Journal, Vol. 3, Iss. 2, pp. 113-120

Robertson, T., (2014). Network Diagnostic Flow Chart-How to Troubleshoot Vehicle Level CAN Communication and CAN Diagnostic Issues on Nissan and Infinity Vehicles, SAE Technical Paper 2014-01-1978

Hu H. and Qin G., (2011). Online Fault Diagnosis for Controller Area Networks, in International Conference on Intelligent Computation Technology and Automation (ICICTA), pp. 452-455, Shenzhen, Guangdong, China

Kelkar S. and Kamal R., (2014). Adaptive Fault Diagnosis Algorithm for Controller Area Network, IEEE

Transactions on Industrial Electronics, Vol. 61, No. 10, pp. 5527-5537

Lei Y., Yuan Y., and Zhao J., (2014). Model-based Detection and Monitoring of the Intermittent Connections for CAN Networks, IEEE Transactions on Industrial Electronics, Vol. 61, No. 6, pp. 2912-2921

Wheeler K., Timucin D., Twombly X., Goebel K., and Wysocki P., (2007). Ageing Aircraft Wiring Fault Detection Survey, NASA Ames Research Center, Moffett Field, CA

Furse C., Smith P., Safavi M., and Lo C., (2005). Feasibility of Spread Spectrum Sensors for Location of Arcs on Live Wires, IEEE Sensors Journal, Vol. 5, No. 6, pp. 1445-1450

Furse C., Chung Y. C., Lo C., and Pendalaya P., (2006). A Critical Comparison of Reflectometry Methods for Location of Wiring Faults, Smart Structures and Systems, Vol. 2, No. 1, pp. 25-46

Zago G. M. and Freitas E. P, (2018). A Quantitative Performance Study on CAN and CAN FD Vehicular Networks, IEEE Transactions on Industrial Electronics, Vol. 65, No. 5

Jiang S., Du X., and Wienckowski N. A., (2015). Method and Apparatus for Open-Wire Fault Detection and Diagnosis in a Controller Area Network, *Patent number: US9568533B2*

Jiang S., Du X., and Nagose A., (2015). Method and Apparatus for Short Fault Isolation in a Controller Area Network, *Patent number: US9678131B2*